Ferroelectric Domain Breakdown

Michel Molotskii,[1] Alex Agronin,[2] Pavel Urenski,[2] Maria Shvebelman,[2] Gil Rosenman,[2,*] and Yossi Rosenwaks[2,†]

[1]*The Wolfson Materials Research Center, Tel Aviv University, Ramat-Aviv, 69978, Israel*
[2]*Department of Electrical Engineering–Physical Electronics, Faculty of Engineering, Tel Aviv University, Ramat-Aviv, 69978, Israel*

(Received 19 September 2002; published 12 March 2003)

We observe a stringlike domain penetration from a ferroelectric surface deep into the crystal bulk induced by a high voltage atomic force microscope tip. The domains, which resemble channels of an electrical breakdown, nucleate under an electric field of around 10^7 V/cm at the ferroelectric surface, and grow throughout the crystal bulk where the external electric field is practically zero. A theory explaining the shape of the formed domains is presented. It shows that the driving force for the domain breakdown is the decrease of the total free energy of the system with increasing domain length.

DOI: 10.1103/PhysRevLett.90.107601 PACS numbers: 77.80.Dj, 07.79.Lh, 68.37.Ps

The key for increasing the degree of miniaturization and integration density of ferroelectric-based microelectronic and photonic devices is the formation of domains with submicron and nanometer lateral dimensions. Such domain structures may be engineered by applying a voltage between an atomic force microscope (AFM) tip and a back electrode of a thin ferroelectric film (see, for example, [1–4]). In these experiments the domain switching is achieved using voltages not exceeding several tens of volts, and the inverted domains have a length comparable with their lateral size. In addition, the domains inverted by low voltage AFM in different bulk ferroelectrics are unstable [3].

We report about the polarization reversal in thick single crystal ferroelectrics occurring under high and strongly inhomogeneous electric field. Such fields are induced by a tip of a high voltage atomic force microscope (HVAFM) developed in our laboratory and capable of applying voltage stresses in the kilovolt range. We show that this superhigh field exceeding the conventional switching fields by 2–3 orders of magnitude induces a new type of domain inversion process.

We have modified a commercial AFM (Autoprobe CP, Thermomicroscopes, Inc.) in order to apply both dc and pulsed bipolar repolarization voltages larger than 5 kV. Ferroelectric domains were tailored in $LiNbO_3$, $RbTiOPO_4$, and $RbTiOAsO_4$ crystals 150–250 μm thick [5]. Local polarization reversal was performed by applying pulsed voltage to a stationary HVAFM tip, and dc voltage was used in the case of fabrication of strip domains where the domains were written by a scanning AFM tip. Similar ferroelectric poling has been observed by Lu *et al.* [6] using electron beam irradiation.

Figure 1(a) shows several ferroelectric domains tailored in $LiNbO_3$ crystal by application of single rectangular voltage pulses ($U = 3.2$ kV, $t \sim 40$ m sec). The domains were imaged using contact electrostatic force microscopy mode [7]. The triangular domain shape has been observed in lithium tantalate, which has similar to lithium niobate ferroelectric properties [8]. Figure 1(b) shows domain strips fabricated in the same $LiNbO_3$ plate. This two-dimensional domain super lattice was written by scanning the HVAFM tip along the polar Z^+ face with a velocity of around 50 μm/ sec. Inspection of the tailored domains by optical microscopy following chemical etching at the opposite polar face showed complete penetration of the domains throughout the crystal bulk. The lateral size of the triangular domains is between 1–1.5 μm [Fig. 1(a)], which is about 2 orders of magnitude smaller than their length. Such domains have a stringlike shape, resembling channels of an electrical breakdown; therefore we call this phenomenon domain breakdown.

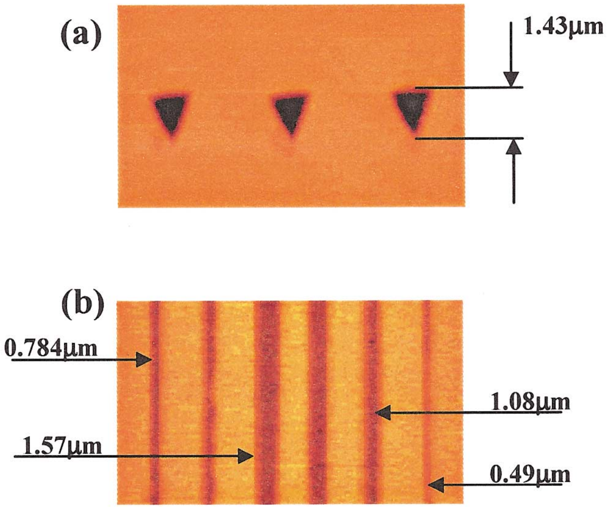

FIG. 1 (color). (a) Ferroelectric domains fabricated in $LiNbO_3$ single crystal (150 μm thick) by application of high voltage pulses ($U = 3.2$ kV, $\tau \sim 40$ m sec) to atomic force microscope tip. (b) Domains inverted in the $LiNbO_3$ by scanning the HVAFM tip along the polar Z^+ face with a velocity of around 50 μm/ sec.

Even though the domain reversal process in HVAFM passes through the same stages as in the conventional low field process, the character of these stages is quite different. The reversal process starts with the nucleation of new domains near the tip. The voltage, of about several kV, applied to the AFM tip generates an electric field exceeding 10^7 V/cm at the ferroelectric polar face. Our calculation, performed in the framework of Landauer's model [9], showed that under such fields the nuclei have quasiatomic dimensions, and the nucleation activation energy does not exceed 10^{-3} eV. The nucleation time decreases to extremely short times of about $\sim 10^{-13}$ s, which is on the order of the lattice vibrations period; therefore the nucleation time is negligibly small relative to the domain breakdown time.

The newly formed domain then expands by motion of the domain walls. This motion is a nonactivated process if the AFM induced field is larger than the coercive field; at this stage the domain size rapidly increases. At larger distances from the tip, where the applied electric field is lower than the coercive field, the domain wall movement is sharply slowed down and becomes thermally activated. The microscopic origin of the activation process in ferroelectrics such as lithium niobate is attributed to the necessity to overcome obstacles during the domain wall motion [10]; the domain walls move until the new domain reaches an equilibrium state.

The most important and unusual effect observed in the HVAFM experiments is the domain forward growth mechanism. In the conventional domain inversion setup using planar switching electrodes, the electric field $\boldsymbol{E}$ is homogeneous throughout the sample. The domain wall movement under homogeneous field $\boldsymbol{E}$ occurs due to the pressure $2(\boldsymbol{E} \cdot \boldsymbol{P}_s)$, where $\boldsymbol{P}_s$ is the spontaneous polarization vector; thus in the case of a zero electric field the driving force for the domain wall motion is zero.

In the case of the high inhomogeneous electric field, the character of the switching process differs significantly. The field of the AFM tip strongly decreases as a function of the distance from the tip apex. We have shown [5] that when the applied voltage is in the kilovolt range, the field decreases from more than 10^7 V/cm at the ferroelectric surface to 10^2 V/cm at a depth of 10 μm, and to only a few V/cm at a depth of 100 μm. The question is, then, what is the driving force for the domain breakdown *in the absence of an external electric field?*

Earlier theories of domain inversion using AFM [1,2,5] cannot explain the observed domain breakdown phenomenon. Kolosov *et al.* [1] assumed that the lateral domain size coincides with the size of the nucleus. The size of the reversed domains was estimated by Durkan *et al.* [2] and Rosenman *et al.* [5], assuming that it is defined by the distance at which the field of the tip and the ferroelectric coercive field are equal. These models can be applied only to the intermediate stages of the domain formation and do not describe the domain final equilibrium state. However, in the case of a long high voltage pulse applied to the HVAFM tip, the newly formed domains have enough time to pass through all the intermediate nonequilibrium stages and reach the final equilibrium state. As it will be shown below, the observed stringlike shape of the domain indeed corresponds to the domain equilibrium state.

The charged AFM tip acts as an active center for the domain nucleation. The active role of charged centers in the formation of new phase nuclei in gases, liquids [11], and solids [12] is well known. A formation of charged particle tracks in the Wilson camera is an example of such a process. These tracks become visible due to an oversaturated steam condensation on the ions created by the charged particles in the steam. The ferroelectric domain nuclei are formed in the vicinity of the AFM tip, in similarity to the liquid drops formed on the ions in the Wilson camera.

Following its formation, the nucleus grows to its equilibrium shape, which is determined by the free energy minimum condition. Our calculation of the potential energy surface (Fig. 2) shows that the growing domain continuously "slides down" to its equilibrium state. It should be emphasized that the existence of the obstacles (pinning defects) affects only the growth kinetics; it does not affect significantly the dimensions of the equilibrated domains.

The domain free energy is composed of three main terms: the energy of the depolarization field W_d created by the bound charges on the domain surface, the surface energy W_s of the domain wall separating the new domain from the surrounding crystal, and the energy of the interaction between the domain and the field of the AFM tip W_t. For the energy calculation we have used the model

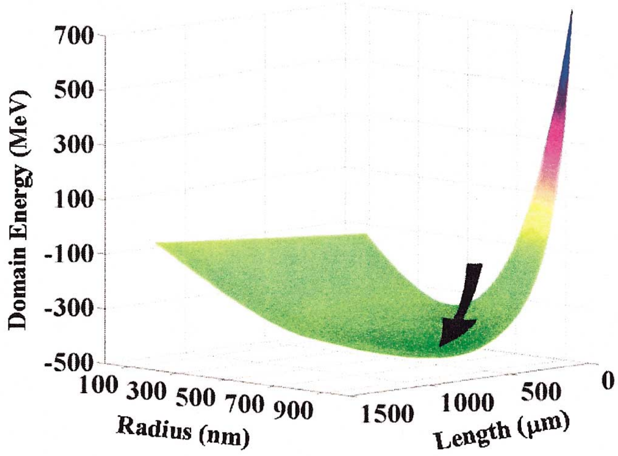

FIG. 2 (color). Potential energy surface of the domain in lithium niobate calculated for a tip voltage of 3.2 kV. In the equilibrium state the length, l_m, of the domain exceeds its radius, r_m, by more than 2 orders of magnitude. The arrow shows the path of the domain transition to the equilibrium state.

proposed by Landauer [9], in which it is assumed that the domain has a semiellipsoidal shape extending in the direction of the polar axis. The values of W_d and W_s for a strongly elongated domain are calculated as [9]

$$W_d = \frac{cr^4}{l}, \quad \text{and} \quad W_s = brl, \tag{1}$$

where

$$c = \frac{16\pi^2 P_s^2}{3\varepsilon_a}\left[\ln\left(\frac{2l}{r}\sqrt{\frac{\varepsilon_a}{\varepsilon_c}}\right) - 1\right], \quad \text{and} \quad b = \frac{\pi^2}{2}\sigma_w.$$

Here r and l are the lengths of the minor and major semiaxes of the semiellipsoid, P_s is the magnitude of the spontaneous polarization, σ_w is the surface energy density, and ε_c and ε_a are the dielectric constants in directions parallel and perpendicular to the polar axis, respectively.

The electric charge on the tip is $q = C_t(U + U_{cpd})$, where C_t is the tip-sample capacitance, U is the voltage applied between the tip and the bottom electrode, and U_{cpd} is the contact potential difference between the sample and the tip (see, e.g., [7]). Since the value of U_{cpd} typically does not exceed 1 V, and the applied voltage U is larger by 3 orders of magnitude, we can neglect below the contribution of the charge $q_{cpd} = C_t U_{cpd} \sim 10^{-3} q$ induced on the tip in the absence of external electric field. It must be emphasized that the applied voltage U leads to the formation of a new equilibrated domain; hence the tip charge, q, calculated above, is due to the *total* electric field in the system including the field of the formed domain. The value of the tip-sample capacitance is calculated within the spherical model (see, for example, [13]). In this model the field of the tip is supposed to coincide with a field of a metallic sphere, the radius of which is equal to the radius of curvature of the tip apex, R. The capacitance of such a sphere in the vicinity of the sample surface has been calculated for the case of an isotropic dielectric [14]. However, since ferroelectrics are anisotropic, the capacitance has to be calculated by substituting $\sqrt{\varepsilon_c \varepsilon_a}$ for ε [15], and in the case of the lithium niobate ($\varepsilon_a = 30$, $\varepsilon_c = 84$), $R = 50$ nm and the distance between the tip apex and the surface $\delta \sim 0.1$ nm the tip-sample capacitance is $C_t = 1.7 \times 10^{-17} F$.

The electric field of the charge $q = C_t U$ was calculated using the formalism reported by Mele [15], which gives for the normal component of the electric field of the tip inside the dielectric:

$$E_n(\rho, z) = \frac{2C_t U}{\gamma(\sqrt{\varepsilon_c \varepsilon_a} + 1)} \frac{(\frac{z}{\gamma} + s)}{[\rho^2 + (\frac{z}{\gamma} + s)^2]^{3/2}}, \tag{2}$$

where ρ and z are cylindrical coordinates and $s = R + \delta$, and $\gamma = \sqrt{\varepsilon_c / \varepsilon_a}$.

It should be emphasized that in our calculations we use values of the dielectric constants ε_c and ε_a measured under low electric fields. We estimate that the contribution of nonlinearity of ferroelectrics, which results in permittivity changes under strong electric fields [16], does not exceed several percent at room temperature. The main reason for this is the small size of the region where the external field is strong compared with the domain size.

When the domain is formed, the value of the spontaneous polarization is changed by $2P_s$. Therefore, the energy of the interaction between the domain and the electric field (2) is

$$W_t = -2\int P_s E_n d^3 r. \tag{3}$$

For an elongated domain ($r \ll l$) Eq. (3) has the form

$$W_t = -f(\sqrt{r^2 + s^2} - s),$$

with effective force acting on the domain

$$f = \frac{8\pi C_t U P_s}{\sqrt{\varepsilon_c \varepsilon_a} + 1}.$$

For small tip-sample distance $s \ll r$, W_t becomes

$$W_t = -fr. \tag{4}$$

Using Eqs. (1) and (4) we obtain for the total energy of the ferroelectric including the following domain:

$$W(r, l) = \frac{cr^4}{l} + brl - fr. \tag{5}$$

The domain equilibrium radius, r_m, and length, l_m, are calculated from the minimum of Eq. (5) to give

$$r_m = \left(\frac{f}{5\sqrt{bc}}\right)^{2/3} \quad \text{and} \quad l_m = \frac{f}{5b}. \tag{6}$$

The domain equilibrium dimensions r_m and l_m depend on the domain surface energy density σ_w. This value has not been measured before for lithium niobate, however it has been reported for lithium tantalate [17]. Using σ_w in the range of 10 to 35 mJ/m^2, and taking into account that in LiNbO$_3$ $\varepsilon_c = 84$, $\varepsilon_a = 30$, and $P_s =$ 75–80 μC/cm^2 we obtain, using Eq. (6) with an applied voltage $U = 3.2$ kV, $r_m = 0.54$–0.83 μm, and $l_m =$ 203–710 μm. Our measured value of the lateral domain size (1–1.5 μm) is within the calculated range $2r_m =$ 1.06–1.66 μm. The calculated value of the equilibrium domain length l_m exceeds the crystal thickness (150 μm); therefore such equilibrium domains indeed will propagate throughout the sample.

We can now explain the domain growth mechanism in the region where the external electric field practically does not exist. The driving force for the domain elongation, F_l, may be found from Eq. (5)

$$F_l = -\frac{\partial W(r, l)}{\partial l} = \frac{cr^4}{l^2} - br. \tag{7}$$

It is seen that the electric field E of the AFM tip does not affect F_l explicitly. The domains are propagating as a result of the decrease in the depolarization field energy, and not due to the direct influence of the tip electric field. The domain elongation continues until forces associated with the increase of the domain surface area compensate the driving force caused by the depolarization field. Evidently, the only reason for the domain elongation is the superhigh field of the AFM tip. However, this effect is indirect; it reveals itself through the increase of the domain radius due to the AFM tip field and a corresponding change of the domain length to satisfy the minimum free energy condition.

The proposed theory of the domain breakdown allows determining the experimental conditions for tailoring stringlike domains in various ferroelectrics. Since b and c are proportional to P_s^2, and f is proportional to P_s, then from Eq. (6) the domain radius varies as $1/P_S^{2/3}$. Therefore, the domain breakdown and the formation of stringlike domains will be observed only in ferroelectrics with high spontaneous polarization. Such is the case in $\mathrm{LiNbO_3}$ where $P_s = 75\text{–}80\ \mu\mathrm{C/cm^2}$, and in $\mathrm{RbTiOPO_4}$ and $\mathrm{RbTiOAsO_4}$, for both of which P_s is a bout 30 $\mu\mathrm{C/cm^2}$. For weak ferroelectrics such as GASH possessing $P_S = 0.35\ \mu\mathrm{C/cm^2}$, and Roshell Salt with $P_S = 0.24\ \mu\mathrm{C/cm^2}$, the spontaneous polarization is smaller by 2 orders of magnitude. Our calculations show that in GASH only thick domains with a diameter 1 order of magnitude larger than that in $\mathrm{LiNbO_3}$ may be tailored under the same experimental conditions. Therefore the phenomenon of domain breakdown cannot take place in weak ferroelectrics.

In summary, we have demonstrated and explained the phenomenon of ferroelectric domain growth under practically zero external electric field in the crystal bulk. Such a growth process is possible only under superhigh inhomogeneous electric fields induced by a point source such as the tip of a high voltage atomic force microscope. We believe that this technology may pave the way for producing high resolution domain superlattices required for future electro-optical devices.

The authors thank E. Glickman and A. Vilenkin for stimulating discussions on the mechanism of the domain breakdown, the financial support of both the Israeli Ministry of Science Culture and Sport, and the Nanoscience and Nanotechnology Center in Tel-Aviv University.

---

*Email address: gilr@eng.tau.ac.il

†Email address: yossir@eng.tau.ac.il

[1] O. Kolosov, A. Gruverman, J. Hatano, K. Takahashi, and H. Tokumoto, Phys. Rev. Lett. **74**, 4309 (1995).

[2] C. Durkan, D. Chu, P. Migliorato, and M. Welland, Appl. Phys. Lett. **76**, 366 (2000).

[3] A. Gruverman, J. Hatano, and H. Tokumoto, Jpn. J. Appl. Phys. **36**, 2207 (1997); L. M. Eng, M. Abplanalp, and P. Günter, Appl. Phys. A **66**, S679 (1998).

[4] R. Ramesh, S. Aggarwal, and O. Ausiello, Mater. Sci. Eng. **R32**, 191 (2001).

[5] G. Rosenman, P. Urenski, A. Agronin, Y. Rosenwaks, and M. Molotskii, Appl. Phys. Lett. **82**, 103 (2003).

[6] H. A. Lu *et al.*, Appl. Phys. Lett. **62**, 1314 (1993).

[7] M. Shvebelman, P. Urenski, R. Shikler, G. Rosenman, Y. Rosenwaks, and M. Molotskii, Appl. Phys. Lett. **80**, 1806 (2002).

[8] V. Gopalan and T. Mitchell, J. Appl. Phys. **85**, 2304 (1999); V. Shur, E. Nikolaeva, E. Shishkin, V. Kozhevnikov, and A. Chernykh, Appl. Phys. Lett. **79**, 3146 (2001).

[9] R. Landauer, J. Appl. Phys. **28**, 227 (1957).

[10] T. J. Yang, V. Gopalan, P. Swart, and U. Mohideen, Phys. Rev. Lett. **82**, 4106 (1999).

[11] A.W. Castleman, Adv. Colloid Interface Sci. **10**, 73 (1979).

[12] A. A. Chernov, *Modern Crystallography. III, Crystal Growth* (Springer-Verlag, Berlin, 1984).

[13] B. D. Terris, J. E. Stern, D. Rugal, and H. J. Mamin, Phys. Rev. Lett. **63**, 2669 (1989).

[14] G. van der Zwan and R. M. Mazo, J. Chem. Phys. **82**, 3344 (1985).

[15] E. J. Mele, Am. J. Phys. **69**, 557 (2001).

[16] F. Jona and G. Shirane, *Ferroelectric Crystals* (Pergamon Press, Oxford, 1962).

[17] V. Gopalan, N. A. Sanford, J. A. Aust, K. Kitamura, and Y. Furukawa, in *Handbook of Advanced Electronic and Photonic Materials and Devices: Ferroelectrics and Dielectrics*, edited by H. S. Nalwa (Academic Press, New York, 2001), Vol. 4, pp. 57–114.